Adıyaman University Journal of Science
https://dergipark.org.tr/en/pub/adyujsci
DergiPark AKADEMİK
ISSN 2147-1630
e-ISSN 2146-586X

Rapid and Specific Purification of RNA by PolyUracil Membranes

Canan ARMUTCU[1,*]

[1]*Hacettepe University, Faculty of Science, Department of Chemistry, TR-06800 Ankara, Turkey*
cananarmutcu@hacettepe.edu.tr, ORCID: 0000-0002-0920-2843

Received: 13.08.2020 **Accepted:** 10.12.2020 **Published:** 30.12.2020

Abstract

Ribonucleic acid (RNA) plays a critically important role in cellular defense, deoxyribonucleic acid (DNA) replication, transcription, and gene expression for living organisms as well as, a lot of diseases such as cancer, immunodeficiency, tumors has been associated with RNA's disruption. For this purpose, supermacropores membranes were designed to purify RNA using nucleotide-based ligand. In this study, polymerizable uracil monomer as uracil methacrylate (UraM) was synthesized, and 2-hydroxyethyl methacrylate (HEMA)-based membranes [poly(HEMA-UraM)] were prepared by bulk polymerization under partially frozen conditions by copolymerization of monomers, UraM, and HEMA. These membranes were characterized via swelling studies, Fourier transform infrared spectroscopy (FTIR), and scanning electron microscopy (SEM). To optimize separation conditions, effects of pH, initial RNA concentration, time, and temperature on RNA adsorption capacity were examined. Maximum adsorption of RNA on poly(HEMA-UraM) membrane was found to be 15.52 mg/g for 0.5 mg/mL RNA initial concentration at 25.0°C with an optimum pH of 7.0. After ten repetitive adsorption-desorption cycles, the RNA adsorption capacity decreased only 3.68%.

Keywords: Membrane; Uracil methacrylate; Nucleotide; Ribonucleic acid; Purification.

* Corresponding Author DOI: 10.37094/adyujsci.780049

PoliUrasil Membranlar ile Hızlı ve Spesifik RNA Saflaştırılması

Öz

Ribonükleik asit (RNA), hücresel savunma, deoksiribonükleik asit (DNA) replikasyonu, transkripsiyon, canlı organizmalar için gen ekspresyonununda önemli bir rol oynar, bunun yanı sıra kanser, immün yetmezlik, tümör gibi birçok hastalık RNA'nın bozulmasıyla ilişkililendirilmiştir. Bu amaçla, RNA saflaştırmak için nükleotid bazlı ligand kullanılarak gözenekli membranlar tasarlanmıştır. Bu çalışmada, polimerize edilebilir urasil monomeri urasil metakrilat (UraM) olarak sentezlenmiş, 2-hidroksietil metakrilat (HEMA) bazlı membranlar [poli(HEMA-UraM)] UraM ve HEMA monomerlerinin kopolimerizasyonu ile kısmen dondurulmuş koşullar altında yığın polimerizasyonu ile hazırlanmıştır. Bu membranlar şişme çalışması, Fourier dönüşümlü kızılötesi spektroskopisi (FTIR) ve taramalı elektron mikroskobu (SEM) ile karakterize edilmiştir. Ayırma koşullarını optimize etmek için, pH, başlangıç RNA konsantrasyonu, süre ve sıcaklığın RNA adsorpsiyon kapasitesi üzerindeki etkileri incelenmiştir. Poli(HEMA-UraM) membranın maksimum RNA adsorpsiyonu 25.0 °C, pH 7.0, 0.5 mg/mL RNA başlangıç derişiminde 15.52 mg/g olduğu bulunmuştur. On tekrarlı adsorpsiyon-desorpsiyon döngüsünden sonra, RNA adsorpsiyon kapasitesi yalnızca %3.68 oranında azaldığı gözlenmiştir.

Anahtar Kelimeler: Membran; Urasil metakrilat; Nükleotid; Ribonükleik asit; Saflaştırma.

1. Introduction

Ribonucleic acid (RNA) plays important roles in heredity and essentially biological processes [1, 2]. There are also some remarkable roles for RNA in biology according to the report from the studies in the last 20 years [3]. The discovery of the RNA features, therapeutic strategy, and the importance of diagnosis lead to purification of RNA with different methods [4-6]. To provide reliable results, RNA purification methods should be highly pure, durable, and provide the production of stable RNA chains.

Many chromatographic techniques have recently been reported for the separation and purifications of biomolecules [7-13]. The traditional techniques still show several disadvantages including the requirement of organic solvents, difficult to scale up, time-consuming, and expensive material [14, 15]. Affinity chromatographic techniques based on the recognition of target molecules using affinity ligand have been developed to overcome these challenges, especially for protein and nucleic acid separation and purification [16, 17]. Affinity chromatography provides using various affinity matrices as solid support can be used to isolate

many kinds of molecules with high selectivity and stability [18, 19]. Thus, this technique eliminates sequential separation steps from a crude medium in one step.

Membranes are three-dimensional polymeric system of interconnected networks of macropores with a size of 10-100 [20, 21]. The large pores and superior flow properties of membranes have allowed these materials to be used in different applications [22]. Membranes also provide easy, fast, and effective elution through their porous structure [23]. Affinity ligands derived from amino acids for using as a functional monomer is an intelligent bio-inspired approach to create a direct biofunctional polymeric network [24]. Herein, nucleotide-based affinity ligands incorporated membrane column was successfully synthesized for the bioseparation of RNA. The presence of membranes composed of nucleotide derivative affinity ligand provides enough specific binding sites and reversible interactions between membranes and RNA.

In the present study, a new approach was developed to investigate rapid and efficient RNA separation in a single step. Firstly, a nucleotide-based functional monomer, the uracil methacrylate (UraM) was synthesized in the presence of methacryloyl chloride and uracil. Secondly, the poly(HEMA-UraM) membranes containing different UraM amounts were obtained by bulk polymerization under partially frozen conditions. Then, Fourier transform infrared (FTIR) spectroscopy, scanning electron microscopy (SEM), and swelling studies were carried out for the characterization of membranes. As finally, the effects of various factors including pH, ligand density, RNA concentration, temperature, and time were investigated to identify the adsorption performance of the adsorbent.

2. Experimental

2.1. Materials

RNA (R6625-25G, Type VI, Torula Yeast), 2-Hydroxyethyl methacrylate (HEMA), ethylene glycol dimethacrylate (EDMA), and sodium dodecyl sulfate (SDS) were obtained from Sigma (St. Louis, MO, USA). Ammonium persulfate (APS), and N,N,N′,N′-tetramethylene diamine (TEMED) were obtained from Merck AG (Darmstadt, Germany). All other chemicals of reagent grade were purchased from Merck AG (Darmstadt, Germany).

2.2. Methods

2.2.1. Synthesis of UraM

The UraM monomer was synthesized according to the literature [24]. Briefly, the uracil (0.01 mol) was dissolved in sodium hydroxide (NaOH) solution (1.0 M). Benzotriazole methacrylate (0.01 mol) and triethylamine (TEA) (0.011 mol) were dissolved in toluene and then this solution was cooled to 0-5ºC. The uracil solution was slowly poured into this solution. This mixture was incubated at room temperature and terminated after 5h. After that, the remaining unreacted TEA and H-benzotriazole were removed out with a vacuum evaporator and functional monomer (uracil methacrylate, UraM) was acquired as an oil-like yellowish solid.

2.2.2. The Synthesis of membranes

Membranes were prepared by bulk polymerization of UraM and 2-hydroxyethyl methacrylate (HEMA) under partially frozen-conditions. Phase I solution contained of HEMA (2.45 mL) and UraM with different amounts (50, 75, or 100 mg UraM) were dissolved in deionized water (2.55 mL). Phase II solution consisted of SDS (0.50 g), and EGDMA (0.6 mL) was dissolved in deionized water (9.40 mL) as an organic phase. Then, both liquid phases were mixed in a magnetic stirrer and then cooled for 20 min. APS (10 mg) and TEMED (50 µL) were mixed into this solution to initiate polymerization. The polymerization was carried out between two glass plates at −12.0ºC for 24 h. After the polymerization was terminated, the poly(HEMA-UraM) membranes thawed at room temperature and were cut with a perforator (6.0 mm in diameter). Afterward, the obtained membranes were washed with deionized water and ethanol until no remaining monomers. Then, membranes were stored in a buffer containing sodium azide (0.1% by weight) to prevent bacterial growth until use. The plain membrane was synthesized via the same polymerization process in the absence UraM monomer as a control.

2.2.3. Characterization of membranes

The water uptake ratios of the membranes were determined by using deionized water [21]. The membranes were lyophilized at -60.0°C using Christ Alpha, 1–2 LD Plus; M Christ GmbH, Germany to get dry weight (w_{dry}). Then, the membranes put into deionized water at ambient temperature for 2 h until they reached a stable wet weight. The membranes were removed from the water, wiped out with filter paper, and reweighed ($w_{swollen}$). The sample weight (dried and wet) were recorded to calculate the membranes water content by means of the below equation:

$$\text{Water uptake ratio } \% = \left[\left(W_{swollen} - W_{dry}\right)/W_{dry}\right] x100 \quad (1)$$

W_{dry} and $W_{swollen}$ are the respective sample weights (g) of membrane before and after water uptake.

The macropores of the membranes was calculated by below equation:

$$\text{Macroporosity } \% = \left[\left(m_{swollen} - m_{squeezed}\right)/m_{swollen}\right] \times 100 \quad (2)$$

Wherein $m_{swollen}$ and $m_{squeezed}$ are the weights (g) of squeezed (after removing free water within macropores) and swollen (after reaching complete swollen state) membranes, respectively.

The poly(HEMA-UraM) membranes were analyzed by FTIR spectrophotometer (Perkin Elmer, Spectrum One, USA) to characterize the functional group. The finely ground membrane samples (2 mg) were dispersed in KBr (98 mg), and turned into a disc form. The FTIR spectrum was recorded over the range of 900- 4000 cm^{-1} wavelengths.

In order to assess the morphology of the membranes, SEM instrument (Tescan, GAIA3, Czech Republic) was utilized from Hacettepe University, Advanced Technologies Application and Research Center (HUNITEK, Ankara, Turkey). The dried membranes were coated with gold and scanned by SEM equipment with different magnifications at high vacuum.

2.2.4. Adsorption/Desorption studies

RNA adsorption experiments were carried out using a batch system in aqueous solution whereas poly(HEMA-UraM) membrane and poly(HEMA) membranes were incubated with appropriate buffer solutions containing RNA solution (1.5 mL) and then incubated for 2 h on a rotator at 100 rpm. The adsorbed RNA amount onto membrane was determined by the measuring UV absorbance of initial and final RNA concentration at 260 nm that was given in the following equation:

$$Q = [(C_i - C_f) \times V]/m \quad (3)$$

where Q, C_i and C_f are adsorbed amount of RNA (mg/g), the initial and final concentrations (mg/mL) of RNA, respectively; V and m are the volume of the aqueous phase (mL), and the mass of the membrane used (g), respectively. The effect of initial RNA concentration (0.025-2.0 mg/mL), pH (4.0-10.0), ligand density (50, 75 and, 100 mg), temperature (4-45 °C), and time (5-120 min) on the binding capacity of the membranes was investigated to determine the optimum RNA adsorption conditions. All experiments were carried out in triplicate within 95% confidence level for all data.

RNA desorption was performed in a batch adsorption process for all membranes. After each adsorption step, adsorbed RNA was eluted using HCl acid solution (0.1 M, 5 mL) at 25°C for 1 h. The successive adsorption-desorption cycle carried out ten times. Finally, the membranes were washed with NaOH solution (50 mM, 5 mL) and deionized water (5 mL) to ready for the next adsorption cycle.

3. Results and Discussion

3.1. Characterization studies

The water uptake capability and mechanical properties of membranes are affiliated to the swelling behavior in an aqueous solution of membrane. Equilibrium swelling degree of poly(HEMA-UraM)-100 membrane was observed to be 5.08 g water/g membrane. Moreover, the equilibrium swelling ratios and macroporosity of membrane was 408% and 77%, respectively. It is demonstrated that the addition of UraM into the polymer structure probably increased the water uptake in aqueous solutions.

FTIR analyses were applied to observe the chemical properties of poly(HEMA-UraM)-100 and poly(HEMA) membranes for evaluating the functional groups (Fig. 1). As seen in FTIR spectra, characteristic bands at 3444 cm^{-1}, and 1716 cm^{-1} were assigned for –OH and -CO stretching, respectively. Additionally, amide I–II bands observed at 1541 cm^{-1} and 1650 cm^{-1} were characteristic bands for UraM which was demonstrated to participate functional monomer successfully in the membrane structure [25].

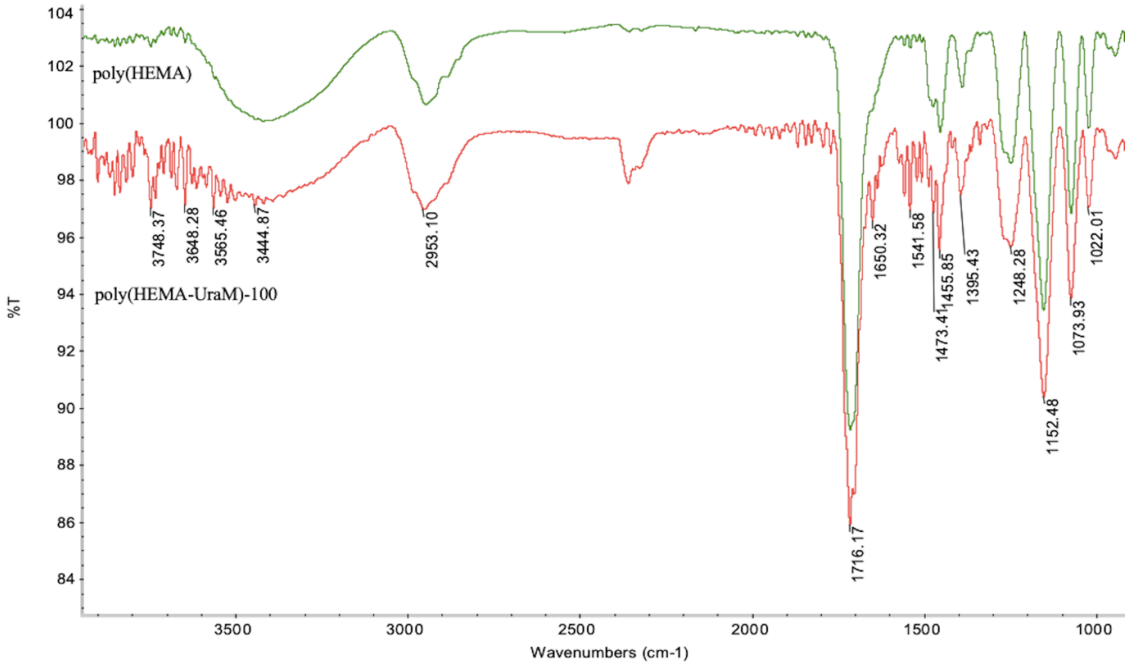

Figure 1: FTIR spectrum of poly(HEMA) and poly(HEMA-UraM)-100 membranes

The SEM images for all membranes were given in Fig. 2. The interconnected macropores, rough surface of the membranes, and also small bead formations are clearly seen in Fig. 2. The different morphological structure of these membranes from the traditional membrane was further verified by SEM images due to the presence of sodium dodecyl sulfate as a surfactant [26]. As

seen in Fig. 2., the synthesized membranes have a unique combination of properties such as interconnected pores of 2– 5 µm size.

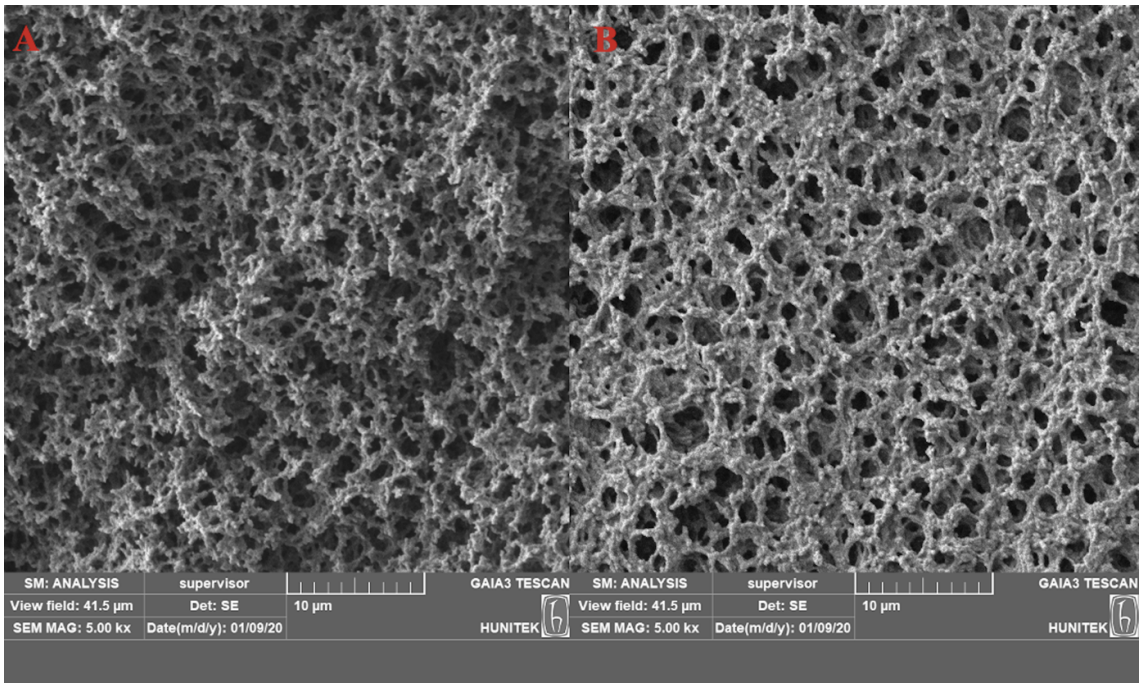

Figure 2: The SEM image of (A) poly(HEMA) and (B) poly(HEMA-UraM)-100 membranes

3.2. RNA Adsorption from aqueous solutions

3.2.1. Effect of pH

The pH effects on RNA adsorption capacity were examined at room temperature for 120 min. RNA adsorption studies were performed at different buffer solutions using acetate (4–5), phosphate (6–8), and carbonate (9-10) buffer systems (Fig. 3). As illustrated in Fig. 3, the maximum RNA binding capacity on poly(HEMA-UraM)-100 membrane was found as 1.91 mg/g at the 0.10 mg/mL initial concentration of RNA in PBS at pH 7.0. At this pH, there are strong hydrogen bonds between the uracil on the polymeric backbone and the adenine in the RNA chain. This effective binding can be explained by the pKa1 (10.01) value of the N3 atom in the uracil and the pka1 (3.88) value of the N1 atom in adenine. At the average of these values (pH: 7.0), they have an optimal charge for H-bonding [26]. Adsorption capacities were reduced at higher and lower this pH value because of the broken of hydrogen bonds between the affinity ligand and RNA chains [27].

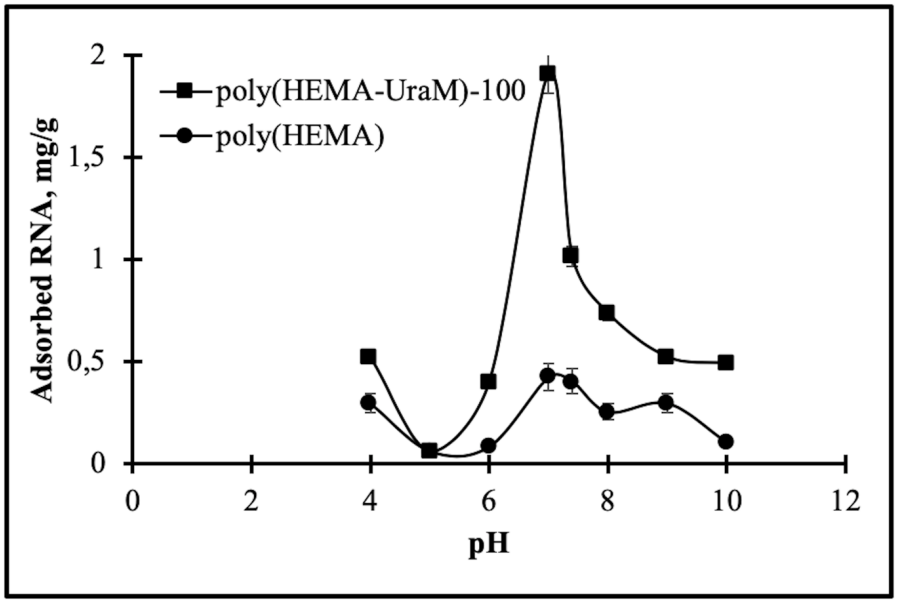

Figure 3: The effect of pH. C_{RNA}: 0.1 mg/mL; time: 120 min; temperature: 25°C

3.2.2. Effect of initial RNA concentration and ligand density

The initial RNA concentration on the adsorption of RNA was investigated at pH 7.0 for 120 min at room temperature. As illustrated in Fig. 4A, the adsorbed RNA amount was increased with an increasing RNA concentration up to 0.75 mg/mL, then remained almost constant. At higher initial concentrations effective active binding sites of membranes were surrounded by RNA and thus, RNA adsorption was reached an equilibrium state.

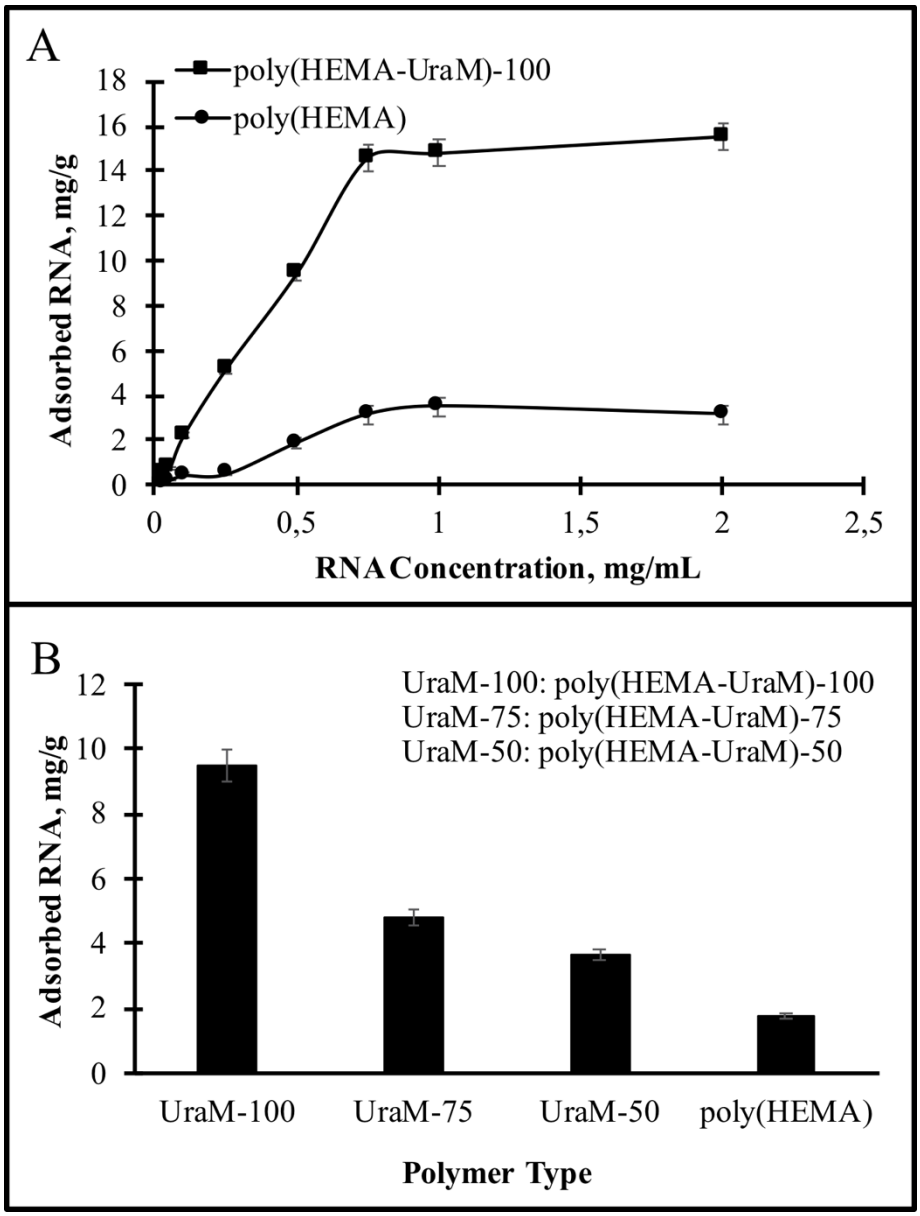

Figure 4: The effect of (A) initial RNA concentration; (B) comparison of RNA adsorption capacities in respect to the amount of functional ligand. pH: 7.0; time: 120 min; temperature: 25°C

The effect of UraM amount was also investigated on the membranes on RNA adsorption. The different UraM amount (50/75/100 mg) in the membranes was analyzed to choose optimal monomer ratio (Fig. 4B). The maximum binding capacities for poly(HEMA-UraM)-50/75/100 membranes were found as 3.66, 4.79, and 9.49 mg/g membrane, respectively. Sufficient number of functional groups play a fundamental role in the recognition of the target molecule and its high adsorption capacity. The results showed that the increasing monomer ratio provided an increase in the adsorption capacity. A negligible amount of RNA adsorption onto the plain poly(HEMA) cryogel was determined. The reason for this negligible binding is that the diffusion of the target molecules into the pores and non-specific interaction [26, 28].

3.2.3. Effect of time

The interaction time on RNA adsorption was investigated by the poly(HEMA) and poly(HEMA-UraM)-100 membranes in the interval of 5–120 min (Fig. 5). The RNA solution can rapidly enter into the large and interconnected porous structures of the membranes. Thus, the adsorption of RNA occurred quite quickly in the first 30 minutes, and then adsorption equilibrium (i.e. plateaus values) were reached within 60 min; that is, the effective binding sites on the membranes were fully occupied and data indicating no significant increase of RNA adsorption. These results confirmed that the poly(HEMA-UraM) membrane showed higher binding capacity for RNA than poly(HEMA) membrane because of the high affinity between ligand and target molecules. These results also supported by occurring of hydrogen bonds between affinity ligand and the target molecule.

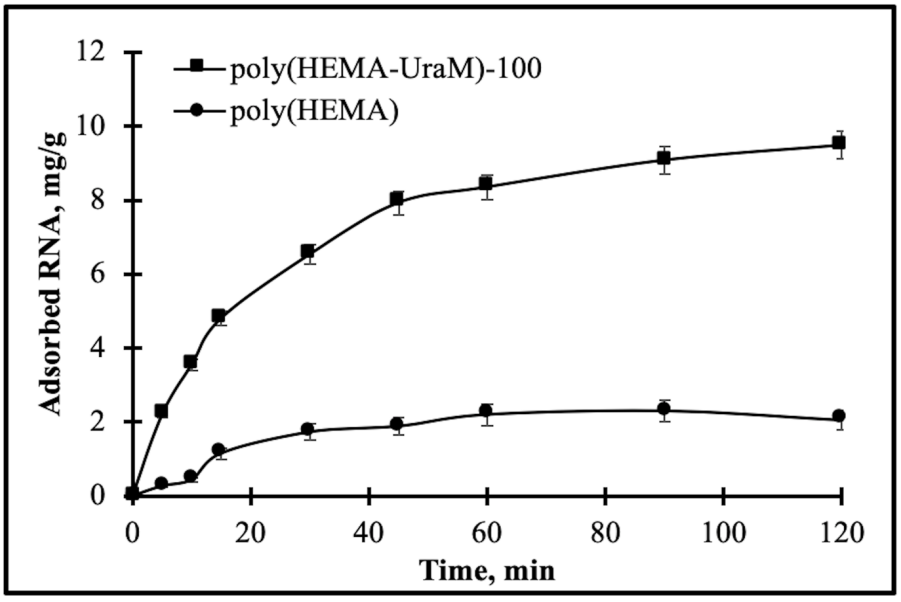

Figure 5: The effect of time. pH: 7.0; C_{RNA}: 0.5 mg/mL; temperature: 25 °C

3.2.4. Effect of temperature

The temperature behavior on the adsorption capacity was performed at different temperatures (4-45°C). As illustrated in Fig. 6, the adsorbed RNA amount was decreased with increasing temperature from 4°C to 45°C. Adsorbed RNA amount reduced from 9.59 mg/g to 8.74 mg/g for poly(HEMA-UraM)-100 membrane by the increasing temperature. The relationship between temperature and RNA adsorption provides important data to determine the basic interactions in the adsorption process. The amount of hydrogen bonds between RNA molecule and UraM monomer may weaken by the increasing temperature. The results also showed that this

strong binding between RNA and poly(HEMA-UraM)-100 membranes mainly rely on hydrogen bonding.

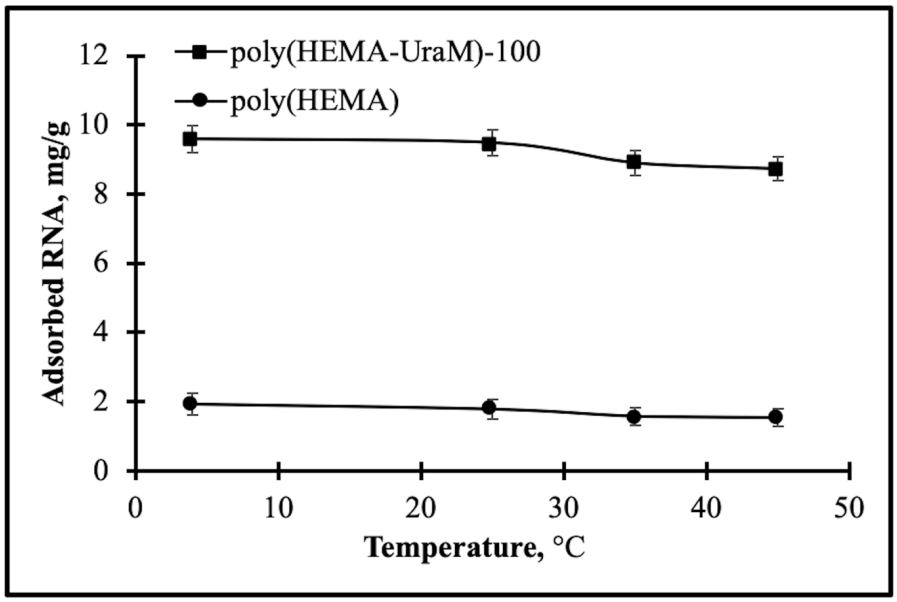

Figure 6: The effect of temperature. pH: 7.0; C_{RNA}: 0.5 mg/mL; time: 120 min

3.3. Adsorption isotherms and kinetic models

Several mathematical isotherm and kinetic models were calculated on the adsorption equilibrium data to describe the RNA adsorption process and surface coverage of adsorbent. Langmuir and Freundlich are frequently investigated methods to define equilibrium adsorption. Flory–Huggins model was also used for the thermodynamic behavior of polymers. The pseudo-first-order, pseudo-second-order, Weber–Morris, and film diffusion models also were examined to kinetic interpretations. In addition, the initial adsorption rate and half adsorption time were calculated. Linearized forms of the equations were given as follows [29-33]:

Adsorption Isotherms at Equilibrium State:

Langmuir $$\frac{1}{Q_{eq}} = \frac{1}{Q_m} + \left(\frac{1}{b.Q_m}\right).\left(\frac{1}{C_{eq}}\right) \quad (4)$$

Freundlich $$\ln Q_{eq} = \ln K_F + \frac{1}{n} \ln C_{eq} \quad (5)$$

Flory-Huggins $$\log\left(\frac{\theta}{C_o}\right) = \log K_{FH} + n_{FH} \log[1-\theta] \quad (6)$$

Where, C_o, C_{eq}, Q_{eq} and Q_m are the concentration of RNA at initial and equilibrium (mg/mL), the amount of RNA adsorbed at equilibrium, and theoretical (mg/g), respectively; θ is

the degree of surface coverage; b, 1/n, K_F, K_{FH}, and n_{FH} are constants of adsorption isotherms, respectively. 1/n shows surface heterogeneity whereas K_{FH} is used to determine Gibbs free energy.

Adsorption Kinetic Modelling:

First order $$\log\left(Q_{eq}-Q_t\right)=\log Q_{eq}-\frac{k_1}{2.303}.t \quad (7)$$

Second order $$\frac{t}{Q_t}=\frac{1}{k_2 Q_{eq}^2}+\frac{t}{Q_{eq}} \quad (8)$$

Weber-Morris (intra-particle diffusion) $$Q_t=k_d t^{0.5}+C_{WM} \quad (9)$$

Initial adsorption rate $$h=k_2 Q_{eq}^2 \quad (10)$$

Half adsorption time $$t_{1/2}=\frac{1}{k_2 Q_{eq}} \quad (11)$$

Film diffusion $$\ln(1-F)=-k_{fd}.t \quad (\text{whereas } F=Q_t/Q_{eq}) \quad (12)$$

Here, k_1 is first order kinetic constant (1/min); k_2 is second order kinetic constant [g/(mg.min)]; k_d is intraparticle diffusion rate constant [g/(mg.min$^{0.5}$)]; Q_{eq} and Q_t are the adsorbed amounts (mg/g) of RNA at t=0 and t=t, respectively [29]. C_{WM} is Weber-Morris constant (mg/g); K_{fd} is the film diffusion constant (1/min).

Table 1: The parameters calculated from adsorption isotherm and kinetic models

Isotherms			Kinetics			
Langmuir			First order			Initial adsorption rate
Q_{max} (mg/g)	b (mL/mg)	R^2	Q_{eq} (mg/g)	k_1 (1/min)	R^2	h (mg/g.min)
29.76	1.307	0.9953	6.57	0.023	0.8023	0.550
Equation: y = 0.0257x + 0.0336			Equation: y = -0.01x + 0.8176			
Freundlich			Second order			Half adsorption rate
K_F	1/n	R^2	Q_{eq} (mg/g)	k_2 (g/mg.min)	R^2	$t_{1/2}$ (min)
17.47	0.8024	0.9339	11.123	$4.49x10^{-3}$	0.9994	20.21
Equation: y = 0.8024x + 2.8603			Equation: y = 0.0899x + 1.8167			
Flory-Huggins			Weber-Morris			Fim diffusion coefficient
K_{FH}	n_{FH}	R^2	k_{id} (g/mg.min$^{0.5}$)	C_{WM}	R^2	k_{fd} (1/min)
158.82	-0,5605	0.7668	0.8396	1.2807	0.8823	0.0343
Equation: y = -0.5605x + 2.2009			Equation: y = 0.8396x + 1.2807			

RNA adsorption isotherms and kinetic data for poly(HEMA-UraM)-100 membrane were given in Table 1. As summarized in Table 1, R^2 value for Langmuir (0.9953) was much higher than Freundlich isotherm (0.9339), and also 1/n value of Freundlich isotherm was calculated as 0.8024 which was also confirming the monolayer adsorption process. According to values of 1/n and R^2, Langmuir isotherm was well-fitted to the adsorption system, as well as, the functional groups (UraM) distribution of the adsorbent surface was energetically homogenous and the adsorption was realized without any diffusion problem and lateral interaction. In addition, Flory–Huggins model was used again to describe the spontaneous nature of adsorption procedure. Gibbs free energy was found as -7.087 kJ/mol using Flory–Huggins equilibrium constant K_{FH} and Gibbs free energy equation ($\Delta G=-RTlnK_{FH}$). As a result, the RNA adsorption was occurred spontaneously due to the required lower energy for the adsorption process [34].

Table 1 displays that calculated R^2 for second-order (0.9994) is higher than first-order kinetic model (0.8023). When the linear correlation coefficients of these models were compared, data was fixed with second-order kinetic model indicating chemical interactions between specific sites of membranes and RNA molecules without any diffusional problems. Furthermore, initial adsorption rate (h), half adsorption rate ($t_{1/2}$),and film diffusion coefficient (k_{fd}) were calculated as 0.550 mg/(g min), 20.21 min, and 0.0343 1/min, respectively. Weber-Morris model is frequently treated as a check whether the intraparticle diffusion and film diffusion are the rate-limiting steps. As illustrated in Table 1, the linear correlation coefficients of Weber-Morris model are lower than the other models. The results show that adsorption process occurred without any diffusion restrictions. This result demonstrated the interconnected macropores structure of membranes having superior flow properties during the adsorption process.

3.4. Desorption and reusability

The development of reusable adsorbent materials is very important in terms of cost-friendly and high stability. For this purpose, the reusability and retained adsorption capacity were investigated using the same membranes. Poly(HEMA-UraM) membrane was used ten times in consequent adsorption-desorption cycles in a batch system using optimal condition, desorbing agent (0.1 M HCl), alkaline solution (5 mM NaOH), and PBS pH 7.0. After the tenth cycle, the adsorbed amount of RNA was found as 9.14 mg/g and maintains 96.32 % of its RNA adsorption capacity (Fig. 7). According to these results, 0.1 M HCl was proved as an appropriate desorption agent. It was demonstrated that RNA could be used many times without no significant decrease for RNA adsorption capacity of the membrane.

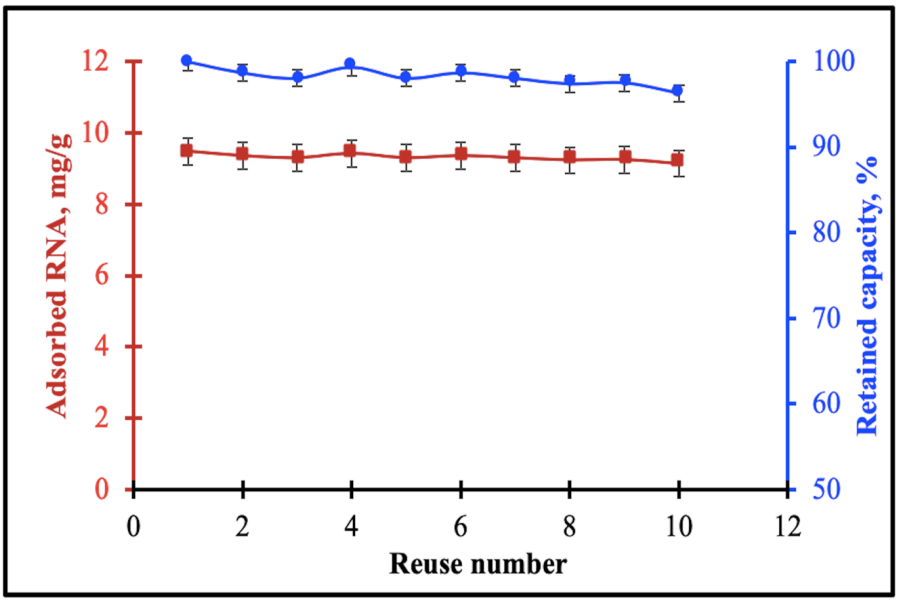

Figure 7: The reusability and retained adsorption capacity. pH: 7.0; C_{RNA}: 0.5 mg/mL; time: 120 min; temperature: 25°C; desorbing agent: 0.1 M HCl

4. Conclusion

The desired feature in affinity chromatography studies is to provide high efficiency RNA adsorption in a short time. Since RNA molecules are hydrolyzed in a short time and also extremely sensitive, there is a growing demand for specific, fast, and efficient RNA separation system. In this context, developed poly(HEMA-UraM) membranes can be classified as a suitable adsorbent due to incorporating a nucleotide into the membrane structure. Herein, polymerizable uracil nucleotide in the polymeric structure ensured to mimic natural Uracil-Adenine interactions which provided high affinity between ligand and target molecules. Moreover, advantages of the bioinspired functional nucleotide with membrane were combined to develop an alternative adsorbent from the structural stability, flow dynamics, and osmotic features of membranes. It was demonstrated that these membranes showed a high reusability performance without significant loss in RNA adsorption capacity. The equilibrium adsorption isotherms fitted well to Langmuir isotherms (R^2 = 0.9953) and the value of adsorption capability (Q_{max}) and equilibrium constant (b) were estimated to be 29.76 mg/g and 1.307 mg/mL for the poly(HEMA-UraM) membrane, respectively. The kinetics of adsorption fitted best to pseudo-second order (R^2 = 0.8023). Finally, the developed membranes promising as a good alternative as supports having high affinity, reusability, and cost-friendly adsorbent.

Acknowledgement

C. Armutcu thanks Sena Piskin, Mirac Tuysuz and Dr. E. Ozgur for their valuable help during the study.

Declaration of conflict of interest

The author has declared no conflict of interest.

References

[1] Sharp, P.A., *The centrality of RNA*, Cell, 136, 577-580, 2009.

[2] Perçin, I., İdil, N., Denizli, A., *RNA purification from Escherichia coli cells using boronated nanoparticles*, Colloids and Surfaces B: Biointerfaces, 162, 146-153, 2018.

[3] Martins, R., Queiroz, J., Sousa, F., *Ribonucleic acid purification*, Journal of Chromatography A, 1355, 1-14, 2014.

[4] Cooper, T.A., Wan, L., Dreyfuss, G., *RNA and disease*, Cell, 136, 777-793, 2009.

[5] Köse, K., Denizli, A., P*oly (hydroxyethyl methacrylate) based magnetic nanoparticles for lysozyme purification from chicken egg white*, Artificial cells, nanomedicine, and biotechnology, 41, 13-20, 2013.

[6] Yang, G., Lu, X., Yuan, L., *LncRNA: a link between RNA and cancer*, Biochimica et Biophysica Acta (BBA)-Gene Regulatory Mechanisms, 1839, 1097-1109, 2014.

[7] Kim, I., Mckenna, S.A., Puglisi, E.V., Puglisi, J.D., *Rapid purification of RNAs using fast performance liquid chromatography (FPLC)*, RNA, 13, 289-294, 2007.

[8] Martins, R., Queiroz, J.A., Sousa, F., *Histidine affinity chromatography-based methodology for the simultaneous isolation of Escherichia coli small and ribosomal RNA*, Biomedical Chromatography, 26, 781-788, 2012.

[9] McGinnis, A.C., Chen, B., Bartlett, M.G., *Chromatographic methods for the determination of therapeutic oligonucleotides*, Journal of Chromatography B, 883, 76-94, 2012.

[10] Romanovskaya, A., Sarin, L.P., Bamford, D.H., Poranen, M.M., *High-throughput purification of double-stranded RNA molecules using convective interaction media monolithic anion exchange columns*, Journal of Chromatography A, 1278, 54-60, 2013.

[11] Vomelova, I., Vaníčková, Z., Šedo, A., *Technical note methods of RNA purification. All ways (should) lead to Rome*, Folia Biologica (Praha), 55, 243-251, 2009.

[12] Warren, W.J., Vella, G., *Principles and methods for the analysis and purification of synthetic deoxyribonucleotides by high-performance liquid chromatography*, Molecular Biotechnology, 4, 179, 1995.

[13] Srivastava, A., Shakya, A.K., Kumar, A., *Boronate affinity chromatography of cells and biomacromolecules using cryogel matrices*, Enzyme and Microbial Technology, 51, 373-381, 2012.

[14] Uhlenbeck, O., *Keeping RNA happy*, RNA, 1, 4, 1995.

[15] Edwards, A.L., Garst, A.D., Batey, R.T., *Determining structures of RNA aptamers and riboswitches by X-ray crystallography, Nucleic Acid and Peptide Aptamers*, Springer2009, pp. 135-163.

[16] Garcia, F., Pires, E., *Recovery processes for biological materials*, Chromatography, Wiley, London, UK, 415-451, 1993.

[17] Scouten, W.H., *Affinity chromatography; bioselective adsorption on inert matrices*, Wiley, NewYork, 1981.

[18] Ayyar, B.V., Arora, S., Murphy, C., O'Kennedy, R., *Affinity chromatography as a tool for antibody purification*, Methods, 56, 116-129, 2012.

[19] Roque, A.C., Silva, C.S., Taipa, M.Â., *Affinity-based methodologies and ligands for antibody purification: advances and perspectives*, Journal of Chromatography A, 1160, 44-55, 2007.

[20] Andaç, M., Tamahkar, E., Denizli, A., *Molecularly imprinted smart cryogels for selective nickel recognition in aqueous solutions*, Journal of Applied Polymer Science, 49746.

[21] Emin Çorman, M., Bereli, N., Özkara, S., Uzun, L., Denizli, A., *Hydrophobic cryogels for DNA adsorption: Effect of embedding of monosize microbeads into cryogel network on their adsorptive performances*, Biomedical Chromatography, 27, 1524-1531, 2013.

[22] Bereli, N., Yavuz, H., Denizli, A., *Protein chromatography by molecular imprinted cryogels*, Journal of Liquid Chromatography & Related Technologies, 1-14, 2020.

[23] Öncel, P., Çetin, K., Topçu, A.A., Yavuz, H., Denizli, A., *Molecularly imprinted cryogel membranes for mitomycin C delivery*, Journal of Biomaterials Science Polymer Edition, 28, 519-531, 2017.

[24] Hur, D., Ekti, S.F., Say, R., *N-Acylbenzotriazole mediated synthesis of some methacrylamido amino acids*, Letters in Organic Chemistry, 4, 585-587, 2007.

[25] Armutcu, C., Çorman, M.E., Bayram, E., Uzun, L., *Purification of Fab and Fc using papain immobilized cryogel bioreactor separator system*, Journal of Chromatography B, 122396, 2020.

[26] Köse, K., Erol, K., Uzun, L., Denizli, A., *PolyAdenine cryogels for fast and effective RNA purification*, Colloids and Surfaces B: Biointerfaces, 146, 678-686, 2016.

[27] Köse, K., Uzun, L., *PolyGuanine methacrylate cryogels for ribonucleic acid purification*, Journal of Separation Science, 39, 1998-2005, 2016.

[28] Çorman, M.E., *Poly-l-lysine modified cryogels for efficient bilirubin removal from human plasma*, Colloids and Surfaces B: Biointerfaces, 167, 291-298, 2018.

[29] Daoud-Attieh, M., Chaib, H., Armutcu, C., Uzun, L., Elkak, A., Denizli, A., *Immunoglobulin G purification from bovine serum with pseudo-specific supermacroporous cryogels*, Separation and Purification Technology, 118, 816-822, 2013.

[30] Foo, K.Y., Hameed, B.H., *Insights into the modeling of adsorption isotherm systems*, Chemical engineering journal, 156, 2-10, 2010.

[31] Sarı, M.M., Armutcu, C., Bereli, N., Uzun, L., Denizli, A., *Monosize microbeads for pseudo-affinity adsorption of human insulin*, Colloids and Surfaces B: Biointerfaces, 84, 140-147, 2011.

[32] Erol, B., Erol, K., Gökmeşe, E., *The effect of the chelator characteristics on insulin adsorption in immobilized metal affinity chromatography*, Process Biochemistry, 83, 104-113, 2019.

[33] Ohale, P.E., Onu, C.E., Ohale, N.J., Obah, S.N., *Adsorptive kinetics, isotherm and thermodynamic analysis of fishpond effluent coagulation using chitin derived coagulant from waste Brachyura shell*, Chemical Engineering Journal Advances, 100036, 2020.

[34] Javadian, H., Ruiz, M., Taghvai, M., Sastre, A.M., *Novel magnetic nanocomposite of calcium alginate carrying poly (pyrimidine-thiophene-amide) as a novel green synthesized polyamide for adsorption study of neodymium, terbium, and dysprosium rare-earth ions*, Colloids and Surfaces A: Physicochemical and Engineering Aspects, 603, 125252, 2020.